

Durham Research Online

Deposited in DRO:

07 May 2008

Version of attached file:

Other

Peer-review status of attached file:

Peer-reviewed

Citation for published item:

Georgiou, G. and Khoze, V. V. (2004) 'Tree amplitudes in gauge theory as scalar MHV diagrams.', Journal of high energy physics., 2004 (05). 070.

Further information on publisher's website:

<http://dx.doi.org/10.1088/1126-6708/2004/05/070>

Publisher's copyright statement:

Additional information:

Use policy

The full-text may be used and/or reproduced, and given to third parties in any format or medium, without prior permission or charge, for personal research or study, educational, or not-for-profit purposes provided that:

- a full bibliographic reference is made to the original source
- a [link](#) is made to the metadata record in DRO
- the full-text is not changed in any way

The full-text must not be sold in any format or medium without the formal permission of the copyright holders.

Please consult the [full DRO policy](#) for further details.

Tree Amplitudes in Gauge Theory as Scalar MHV Diagrams

George Georgiou and Valentin V. Khoze

*Centre for Particle Theory, Department of Physics and IPPP,
University of Durham, Durham, DH1 3LE, UK*

`george.georgiou, valya.khoze@durham.ac.uk`

Abstract

It was proposed in hep-th/0403047 that all tree amplitudes in pure Yang-Mills theory can be constructed from known MHV amplitudes. We apply this approach for calculating tree amplitudes of gauge fields and fermions and find agreement with known results. The formalism amounts to an effective scalar perturbation theory which offers a much simpler alternative to the usual Feynman diagrams in gauge theory and can be used for deriving new simple expressions for tree amplitudes. At tree level the formalism works in a generic gauge theory, with or without supersymmetry, and for a finite number of colours.

1 Introduction

In a recent paper [1] Witten outlined a construction which interprets perturbative amplitudes of conformal $\mathcal{N} = 4$ supersymmetric gauge theory as D-instanton contributions in a topological string theory in twistor space. Motivated by this correspondence, Cachazo, Svrcek and Witten [2] proposed a remarkable new approach for calculating all tree-level amplitudes of n gluons. In this approach tree amplitudes in a pure gauge theory are found by summing tree-level scalar Feynman diagrams with new vertices. The building blocks of this formalism are scalar propagators $1/p^2$, and tree-level maximal helicity violating (MHV) amplitudes, which are interpreted as new scalar vertices. Using multi-particle amplitudes as effective vertices enables one to save dramatically on a number of permutations in usual Feynman diagrams.

The new perturbation theory involves scalar diagrams since MHV vertices are scalar quantities. They are linked together by scalar propagators at tree-level, and the internal lines are continued off-shell in a particular fashion. The final result for any particular amplitude can be shown to be Lorentz-covariant and is independent of a particular choice for the off-shell continuation. The authors of [2] derived new expressions for a class of tree amplitudes with three negative helicities and any number of positive ones. It has been verified in [2] and [3] that the new scalar graph approach agrees with a number of known conventional results for scattering amplitudes in pure gauge theory

The motivation of this note is to apply the new diagrammatic approach of [2] to tree amplitudes which involve fermion fields as well as gluons. In the presence of fermions there are two new classes of MHV vertices, which involve one and two quark-antiquark lines. This is in addition to the single class of purely gluonic MHV vertices considered in [2]. All three classes of vertices can in principle be connected to one another via propagators at tree level. This leads to new diagrams and provides us with useful tests of the method. Confirmation of the new diagrammatic approach of [2] in more general settings is important for two reasons. First, as mentioned earlier, this approach offers a much simpler alternative to the usual Feynman diagrams in gauge theory and can be used for deriving a variety of new closed-form expressions for multi-parton tree amplitudes. Of course, in practice, in deriving multi-parton amplitudes there is no need to calculate Feynman diagrams directly as there are other powerful techniques based on the recursion relations [4, 5]. We also note that scalar graphs as a powerful method for calculating amplitudes in field theories with gauge fields and fermions was introduced already in [6].¹

¹In the approach of [6] one also works in the helicity basis and uses scalar propagators and scalar

Our second reason for studying and generalising this approach is its relation to string theory in twistor space. On the string side, the SYM amplitude is interpreted in [1] as coming from a D-instanton of charge d , where d is equal to the number of negative helicity particles minus 1 plus the number of loops. The new scalar graph method of [2] is interpreted on the string side as the contribution coming entirely from d single instantons. On the other hand, in an interesting recent paper [7] it is argued that the SYM amplitude is fully determined by the opposite extreme case – a single d -instanton. In principle, there are also contributions from a mixed set of connected and disconnected instantons of total degree d .

From the gauge theory perspective, there are two questions we can ask:

(1) does the scalar formalism of [2] correctly incorporate gluinos in a generic supersymmetric theory, and

(2) does it work for diagrams with fundamental quarks in a non-supersymmetric $SU(N)$ theory, i.e. in QCD?

It is often stated in the literature that any gauge theory is supersymmetric at tree level. This is because at tree level superpartners cannot propagate in loops. This observation, on its own, does not answer the question of how to relate amplitudes with quarks to amplitudes with gluinos. The colour structure of these amplitudes is clearly different.² However, we will see that the purely kinematic parts of these amplitudes are the same at tree level.

In the next section we briefly recall well-known results about decomposition of full amplitudes into the colour factor T_n and the purely kinematic partial amplitude A_n . A key point in the approach of [2] and also in [1, 7] is that only the kinematic amplitude A_n is evaluated directly. Since A_n does not contain colour factors, it is the same for tree amplitudes involving quarks and for those with gluinos. There is an important point we should stress here. Apriori, when comparing kinematic amplitudes in a non-supersymmetric and in a supersymmetric theory, we should make sure that both theories have a similar field content. In particular, when comparing kinematic amplitudes in QCD and in SYM, (at least initially) we need to restrict to the SYM theory with vectors, fermions and no scalars. Scalars are potentially dangerous, since they can propagate in

vertices. However the scalar vertices utilized in [6] are not the MHV vertices used in [2] and here. We thank Warren Siegel for drawing our attention to Ref. [6].

²Also, amplitudes with gluons and gluinos are automatically planar at tree level. This is not the case for tree diagrams with quarks, as they do contain $1/N$ -suppressed terms in $SU(N)$ gauge theory.

the internal lines and spoil the agreement between the amplitudes. Hence, while the kinematic tree-level amplitudes in massless QCD agree with those in $\mathcal{N} = 1$ pure SYM, one might worry that the agreement will be lost when comparing QCD with $\mathcal{N} = 4$ (and $\mathcal{N} = 2$) theories. Fortunately, this is not the case, the agreement between amplitudes in QCD and amplitudes in SYM theories does not depend on \mathcal{N} . The main point here is that in $\mathcal{N} = 2$ and $\mathcal{N} = 4$ theories, the scalars ϕ couple to gluinos Λ^A and Λ^B from different $\mathcal{N} = 1$ supermultiplets,

$$S_{\text{Yukawa}} = g_{\text{YM}} \text{tr} \Lambda_A^- [\phi^{AB}, \Lambda_B^-] + g_{\text{YM}} \text{tr} \Lambda^{A+} [\bar{\phi}_{AB}, \Lambda^{B+}] , \quad (1.1)$$

where $A, B = 1, \dots, \mathcal{N}$, and $\phi^{AB} = -\phi^{BA}$, hence $A \neq B$. At the same time, in the kinematic amplitudes quarks are identified with gluinos of the same fixed A , i.e.

$$q \leftrightarrow \Lambda^{A=1+}, \bar{q} \leftrightarrow \Lambda_{A=1}^-.$$

QCD-amplitudes with m quarks, m antiquarks and l gluons in external lines correspond to SYM-amplitudes with m gluinos Λ^{1+} , m anti-gluinos Λ_1^- , and l gluons. Since all external (anti)-gluinos are from the same $\mathcal{N} = 1$ supermultiplet, they cannot produce scalars in the internal lines of tree diagrams. These diagrams are the same for all $\mathcal{N} = 0, \dots, 4$. Of course, in $\mathcal{N} = 4$ and $\mathcal{N} = 2$ theories there are other classes of diagrams with gluinos from different $\mathcal{N} = 1$ supermultiplets, and also with scalars in external lines. Applications of the scalar graph approach to these more general classes of tree amplitudes in $\mathcal{N} = 2, 4$ will be presented in [8].

We conclude that, if the new formalism gives correct results for partial amplitudes A_n in a supersymmetric theory, it will also work in a nonsupersymmetric case, and for a finite number of colours. Full amplitudes are then determined uniquely from the kinematic part A_n , and the known expressions for T_n , given in (2.3), (2.5) below. This means that for tree amplitudes questions (1) and (2) are essentially the same.

In section 3 we explain how the diagrammatic approach of [2] works for calculating scattering amplitudes of gluons and fermions at tree level. This method leads to explicit and relatively simple expressions for many amplitudes. As a first example, using the scalar graph approach, we derive an expression for non-MHV $--- + \dots +$ amplitudes A_n with two fermions and $n - 2$ gluons. We furthermore derive a non-MHV n -point amplitude which involves four fermions. These new results are checked successfully against some previously known expressions for $n = 4, 5$.

In section 4 we outline some obvious conceptual difficulties in addressing loop contributions to n -point amplitudes in a massless gauge theory without an infrared cutoff.

2 Tree Amplitudes

We concentrate on tree-level amplitudes in a gauge theory with an arbitrary finite number of colours. For definiteness we take the gauge group to be $SU(N)$ and consider tree-level scattering amplitudes with arbitrary numbers of external gluons and fermions (it is also straightforward to include scalar fields, but we leave them out from most of what follows for simplicity). $SU(N)$ is unbroken and all fields are taken to be massless, we refer to them generically as gluons, gluinos and quarks, though the gauge theory is not necessarily assumed to be supersymmetric.

2.1 Colour decomposition

It is well-known that a full n -point amplitude \mathcal{M}_n can be represented as a sum of products of colour factors T_n and purely kinematic partial amplitudes A_n ,

$$\mathcal{M}_n(\{k_i, h_i, c_i\}) = \sum_{\sigma} T_n(\{c_{\sigma(i)}\}) A_n(\{k_{\sigma(i)}, h_{\sigma(i)}\}). \quad (2.1)$$

Here $\{c_i\}$ are colour labels of external legs $i = 1 \dots n$, and the kinematic variables $\{k_i, h_i\}$ are on-shell external momenta and helicities: all $k_i^2 = 0$, and $h_i = \pm 1$ for gluons, $h_i = \pm \frac{1}{2}$ for fermions. The sum in (2.1) is over appropriate simultaneous permutations σ of colour labels $\{c_{\sigma(i)}\}$ and kinematic variables $\{k_{\sigma(i)}, h_{\sigma(i)}\}$. The colour factors T_n are easy to determine, and the non-trivial information about the full amplitude \mathcal{M}_n is contained in the purely kinematic part A_n . If the partial amplitudes $A_n(\{k_i, h_i\})$ are known for all permutations σ of the kinematic variables, the full amplitude \mathcal{M}_n can be determined from (2.1).

We first consider tree amplitudes with arbitrary numbers of gluons and gluinos (and with no quarks). The colour variables $\{c_i\}$ correspond to the adjoint representation indices, $\{c_i\} = \{a_i\}$, and the colour factor T_n is a single trace of generators,

$$\mathcal{M}_n^{\text{tree}}(\{k_i, h_i, a_i\}) = \sum_{\sigma} \text{tr}(T^{a_{\sigma(1)}} \dots T^{a_{\sigma(n)}}) A_n^{\text{tree}}(k_{\sigma(1)}, h_{\sigma(1)}, \dots, k_{\sigma(n)}, h_{\sigma(n)}). \quad (2.2)$$

Here the sum is over $(n-1)!$ noncyclic inequivalent permutations of n external particles. The single-trace structure in (2.2),

$$T_n = \text{tr}(T^{a_1} \dots T^{a_n}), \quad (2.3)$$

implies that all tree level amplitudes of particles transforming in the adjoint representation of $SU(N)$ are planar. This is not the case neither for loop amplitudes, nor for tree amplitudes involving fundamental quarks.

Fields in the fundamental representation couple to the trace $U(1)$ factor of the $U(N)$ gauge group. In passing to the $SU(N)$ case this introduces power-suppressed $1/N^p$ terms. However, there is a remarkable simplification for tree diagrams involving fundamental quarks: the factorisation property (2.1) still holds. More precisely, for a fixed colour ordering σ , the amplitude with m quark-antiquark pairs and l gluons (and gluinos) is still a perfect product,

$$T_{l+2m}(\{c_{\sigma(i)}\}) A_{l+2m}(\{k_{\sigma(i)}, h_{\sigma(i)}\}), \quad (2.4)$$

and all $1/N^p$ corrections to the amplitude are contained in the first term. For tree amplitudes the exact colour factor in (2.4) is [9]

$$T_{l+2m} = \frac{(-1)^p}{N^p} (T^{a_1} \dots T^{a_{l_1}})_{i_1 \alpha_1} (T^{a_{l_1+1}} \dots T^{a_{l_2}})_{i_2 \alpha_2} \dots (T^{a_{l_{m-1}+1}} \dots T^{a_l})_{i_m \alpha_m}. \quad (2.5)$$

Here l_1, \dots, l_m correspond to an arbitrary partition of an arbitrary permutation of the l gluon indices; i_1, \dots, i_m are colour indices of quarks, and $\alpha_1, \dots, \alpha_m$ – of the antiquarks. In perturbation theory each external quark is connected by a fermion line to an external antiquark (all particles are counted as incoming). When quark i_k is connected by a fermion line to antiquark α_k , we set $\alpha_k = \bar{i}_k$. Thus, the set of $\alpha_1, \dots, \alpha_m$ is a permutation of the set $\bar{i}_1, \dots, \bar{i}_m$. Finally, the power p is equal to the number of times $\alpha_k = \bar{i}_k$ minus 1. When there is only one quark-antiquark pair, $m=1$ and $p=0$. For a general m , the power p in (2.5) varies from 0 to $m - 1$.

The kinematic amplitudes A_{l+2m} in (2.4) have the colour information stripped off and hence do not distinguish between fundamental quarks and adjoint gluinos. Thus,

$$A_{l+2m}(q, \dots, \bar{q}, \dots, g^+, \dots, g^-, \dots) = A_{l+2m}(\Lambda^+, \dots, \Lambda^-, \dots, g^+, \dots, g^-, \dots), \quad (2.6)$$

where $q, \bar{q}, g^\pm, \Lambda^\pm$ denote quarks, antiquarks, gluons and gluinos of \pm helicity.

In section 3 we will use the scalar graph formalism of [2] to evaluate the kinematic amplitudes A_n in (2.6). Full amplitudes can then be determined uniquely from the kinematic part A_n , and the known expressions for T_n in (2.3) and (2.5) by summing over the inequivalent colour orderings in (2.1).

From now on we concentrate on the purely kinematic part of the amplitude, A_n .

2.2 Helicity amplitudes

We will be studying tree level partial amplitudes $A_n = A_{l+2m}$ with l gluons and $2m$ fermions in the helicity basis. All external lines are defined to be incoming, and a fermion

of helicity $+\frac{1}{2}$ is always connected by a fermion propagator to a helicity $-\frac{1}{2}$ fermion,³ hence the number of fermions $2m$ is always even.

A tree amplitude A_n with n or $n-1$ particles of positive helicity vanishes identically. The same is true for A_n with n or $n-1$ particles of negative helicity. First nonvanishing amplitudes contain $n-2$ particles with helicities of the same sign and are called maximal helicity violating (MHV) amplitudes.

The spinor helicity formalism⁴ is defined in terms of two commuting spinors of positive and negative chirality, λ_a and $\tilde{\lambda}_{\dot{a}}$. Using these spinors, any on-shell momentum of a massless particle, $p_\mu p^\mu = 0$, can be written as

$$p_{a\dot{a}} = p_\mu \sigma^\mu = \lambda_a \tilde{\lambda}_{\dot{a}} . \quad (2.7)$$

Spinor inner products are introduced as

$$\langle \lambda, \lambda' \rangle = \epsilon_{ab} \lambda^a \lambda'^b , \quad [\tilde{\lambda}, \tilde{\lambda}'] = \epsilon_{\dot{a}\dot{b}} \tilde{\lambda}^{\dot{a}} \tilde{\lambda}'^{\dot{b}} . \quad (2.8)$$

Then a scalar product of two null vectors, $p_{a\dot{a}} = \lambda_a \tilde{\lambda}_{\dot{a}}$ and $q_{a\dot{a}} = \lambda'_a \tilde{\lambda}'_{\dot{a}}$, is

$$p_\mu q^\mu = \frac{1}{2} \langle \lambda, \lambda' \rangle [\tilde{\lambda}, \tilde{\lambda}'] . \quad (2.9)$$

Momentum conservation in an n -point amplitude provides another useful identity

$$\sum_{i=1}^n \langle \lambda_r \lambda_i \rangle [\tilde{\lambda}_i \tilde{\lambda}_s] = 0 , \quad (2.10)$$

for arbitrary $1 \leq r, s \leq n$.

In the usual perturbative evaluation of amplitudes, external on-shell lines in Feynman diagrams are multiplied by wave-function factors: a polarization vector ε_\pm^μ for each external gluon A_μ , and spinors u_\pm and \bar{u}_\pm for external quarks and antiquarks. The resulting amplitude is a Lorentz scalar. The spinors λ and $\tilde{\lambda}$ are precisely the wave-functions of fermions and corresponding antifermions (see Appendix for more detail)

$$u_+(k_i)_a = \lambda_{ia} , \quad \overline{u_+(k_i)}_{\dot{a}} = \tilde{\lambda}_{i\dot{a}} , \quad (2.11)$$

³This is generally correct only in theories without scalar fields. In the $\mathcal{N} = 4$ theory, a pair of positive helicity fermions, Λ^{1+} , Λ^{2+} , can be connected to another pair of positive helicity fermions, Λ^{3+} , Λ^{4+} , by a scalar propagator. As already mentioned in the introduction, for all amplitudes considered in this paper we will take external fermions from the same $\mathcal{N} = 1$ supermultiplet, i.e. $A = 1$, and this will rule out contributions of scalar fields even in the $\mathcal{N} = 4$ theory.

⁴This formalism was used for calculating scattering amplitudes first in [10, 11, 4]. We follow conventions of [1] and refer the reader also to comprehensive reviews [9, 12] where more detail and references can be found. Our helicity spinor conventions are summarised in the Appendix

and the polarization vectors ε_{\pm}^{μ} are also defined in a natural way in terms of $\lambda, \tilde{\lambda}$ (and a ‘reference’ spinor), as in [1].

$A_n(g_1^+, \dots, g_{r-1}^+, g_r^-, g_{r+1}^+, \dots, g_{s-1}^+, g_s^-, g_{s+1}^+, \dots, g_n^+)$ is the ‘mostly plus’ purely gluonic MHV amplitude with $n - 2$ gluons of positive helicity and 2 gluons of negative helicity in positions r and s . To simplify notation, from now on we will not indicate the positive helicity gluons in the mostly plus amplitudes and the negative helicity gluons in the mostly minus amplitudes. Also, the mostly plus maximal helicity violating amplitudes will be referred to simply as the MHV amplitudes, and the mostly minus maximal helicity violating amplitudes will be called the $\overline{\text{MHV}}$. Finally, in all the amplitudes A_n we will suppress the common momentum conservation factor of

$$i g_{\text{YM}}^{n-2} (2\pi)^4 \delta^{(4)} \left(\sum_{i=1}^n \lambda_{ia} \tilde{\lambda}_{i\dot{a}} \right) \quad (2.12)$$

Using these conventions, the MHV gluonic amplitude is

$$A_n(g_r^-, g_s^-) = \frac{\langle \lambda_r, \lambda_s \rangle^4}{\prod_{i=1}^n \langle \lambda_i, \lambda_{i+1} \rangle} \equiv \frac{\langle r \ s \rangle^4}{\prod_{i=1}^n \langle i \ i+1 \rangle} , \quad (2.13)$$

where $\lambda_{n+1} \equiv \lambda_1$. The corresponding $\overline{\text{MHV}}$ amplitude with positive helicity gluons in positions r and s is

$$A_n(g_r^+, g_s^+) = \frac{[\tilde{\lambda}_r, \tilde{\lambda}_s]^4}{\prod_{i=1}^n [\tilde{\lambda}_i, \tilde{\lambda}_{i+1}]} \equiv \frac{[r \ s]^4}{\prod_{i=1}^n [i \ i+1]} . \quad (2.14)$$

The closed-form expressions (2.13), (2.14) were derived in [11, 4]. These and other results in the helicity formalism are reviewed in [9, 12].

An MHV amplitude $A_n = A_{l+2m}$ with l gluons and $2m$ fermions (from the same $\mathcal{N} = 1$ supermultiplet) exists only for $m = 0, 1, 2$. This is because it must have precisely $n - 2$ particles with positive and 2 with negative helicities, and our fermions always come in pairs with helicities $\pm \frac{1}{2}$. Hence, including (2.13), there are three types of MHV tree amplitudes,

$$A_n(g_r^-, g_s^-) , \quad A_n(g_t^-, \Lambda_r^-, \Lambda_s^+) , \quad A_n(\Lambda_t^-, \Lambda_s^+, \Lambda_r^-, \Lambda_q^+) . \quad (2.15)$$

Expressions for all three MHV amplitudes in (2.15) can be simply read off the $\mathcal{N} = 4$ supersymmetric formula of Nair [13]:

$$A_n^{\mathcal{N}=4} = \delta^{(8)} \left(\sum_{i=1}^n \lambda_{ia} \eta_i^A \right) \frac{1}{\prod_{i=1}^n \langle i \ i+1 \rangle} , \quad (2.16)$$

where η_i^A , $A = 1, 2, 3, 4$ is the $\mathcal{N} = 4$ Grassmann coordinate. Taylor expanding (2.16) in powers of η_i , one can identify each term in the expansion with a particular tree-level MHV amplitude in the $\mathcal{N} = 4$ theory. $(\eta_i)^k$ for $k = 0, \dots, 4$ is interpreted as the i^{th} particle with helicity $h_i = 1 - \frac{k}{2}$. Hence, $h_i = \{1, \frac{1}{2}, 0, -\frac{1}{2}, -1\}$, where zero is the helicity of a scalar field. It is straightforward to write down a general rule for associating a power of η with all component fields in $\mathcal{N} = 4$,

$$\begin{aligned} g_i^- &\leftarrow \eta_i^1 \eta_i^2 \eta_i^3 \eta_i^4, \quad \phi^{AB} \leftarrow \eta_i^A \eta_i^B, \quad \Lambda^{A+} \leftarrow \eta_i^A, \quad g_i^- \leftarrow 1, \\ \Lambda_1^- &\leftarrow -\eta_i^2 \eta_i^3 \eta_i^4, \quad \Lambda_2^- \leftarrow -\eta_i^1 \eta_i^3 \eta_i^4, \quad \Lambda_3^- \leftarrow -\eta_i^1 \eta_i^2 \eta_i^4, \quad \Lambda_4^- \leftarrow -\eta_i^1 \eta_i^2 \eta_i^3. \end{aligned} \quad (2.17)$$

The amplitude (2.13) can be obtained from (2.16), (2.17) by selecting the $(\eta_r)^4 (\eta_s)^4$ term; the second amplitude in (2.15) follows an appropriate $(\eta_t)^4 (\eta_r)^3 (\eta_s)^1$ term in (2.16); and the third amplitude in (2.15) is an $(\eta_r)^3 (\eta_s)^1 (\eta_p)^3 (\eta_q)^1$ term. For our calculations in addition to (2.13) we will need expressions for MHV amplitudes with $m = 1$ and $m = 2$ pairs of fermions (with the same A). The MHV amplitude with two external fermions and $n - 2$ gluons is

$$A_n(g_t^-, \Lambda_r^-, \Lambda_s^+) = \frac{\langle t r \rangle^3 \langle t s \rangle}{\prod_{i=1}^n \langle i i+1 \rangle}, \quad A_n(g_t^-, \Lambda_s^+, \Lambda_r^-) = -\frac{\langle t r \rangle^3 \langle t s \rangle}{\prod_{i=1}^n \langle i i+1 \rangle}, \quad (2.18)$$

where the first expression corresponds to $r < s$ and the second to $s < r$ (and t is arbitrary). The MHV amplitudes with four fermions and $n - 4$ gluons on external lines are

$$A_n(\Lambda_t^-, \Lambda_s^+, \Lambda_r^-, \Lambda_q^+) = \frac{\langle t r \rangle^3 \langle s q \rangle}{\prod_{i=1}^n \langle i i+1 \rangle}, \quad A_n(\Lambda_t^-, \Lambda_r^-, \Lambda_s^+, \Lambda_q^+) = -\frac{\langle t r \rangle^3 \langle s q \rangle}{\prod_{i=1}^n \langle i i+1 \rangle} \quad (2.19)$$

The first expression in (2.19) corresponds to $t < s < r < q$, the second – to $t < r < s < q$, and there are other similar expressions, obtained by further permutations of fermions, with the overall sign determined by the ordering.

The $\overline{\text{MHV}}$ amplitude can be obtained, as always, by exchanging helicities $+ \leftrightarrow -$ and $\langle i j \rangle \leftrightarrow [i j]$. Expressions (2.18), (2.19) can also be derived from $\mathcal{N} = 1$ supersymmetric Ward identities, as in [9, 12].

All amplitudes following from Nair's general expression (2.16) are analytic in the sense that they depend only on $\langle \lambda_i \lambda_j \rangle$ spinor products, and not on $[\tilde{\lambda}_i \tilde{\lambda}_j]$. These include amplitudes in (2.13), (2.18), (2.19), as well as more complicated classes of amplitudes, i.e. with external gluinos Λ^A , $\Lambda^{B \neq A}$, etc, and with external scalar fields. These extra classes of analytic amplitudes, interpreted as vertices in the scalar graph approach, are being investigated in [8] and will not be discussed here further.

3 Calculating Amplitudes Using Scalar Graphs

The formalism of [2] represents all non-MHV tree amplitudes (including $\overline{\text{MHV}}$) as sums of tree diagrams in an effective scalar perturbation theory. The vertices in this theory are the MHV amplitudes (2.15), continued off-shell as described below, and connected by scalar bosonic propagators $1/p^2$.

An obvious question one might ask is why one should use the $1/p^2$ propagator when connecting fermion lines in MHV vertices (2.15). To answer this, recall that the vertices (2.15) already contain the wave-function factors for all external lines, including fermions (2.11). An incoming fermion in one MHV vertex, connected by $1/p^2$ to an incoming antifermion of another MHV vertex, corresponds to a factor of

$$u_+(p)_a \frac{1}{p^2} \overline{u_+(p)}_{\dot{a}} = \frac{\not{p}_{a\dot{a}}}{p^2} , \quad (3.1)$$

for an internal line in the usual Feynman diagram, which is just the right answer. There is a subtlety with choosing the ordering of fermions in each vertex which is explained in Appendix in equations (4.5) and (4.7).

When one leg of an MHV vertex is connected by a propagator to a leg of another MHV vertex, both of these legs become internal to the diagram and have to be continued off-shell. Off-shell continuation is defined as follows [2]: we pick an arbitrary spinor $\eta^{\dot{a}}$ and define λ_a for any internal line carrying momentum $p_{a\dot{a}}$ by

$$\lambda_a = p_{a\dot{a}} \eta^{\dot{a}} . \quad (3.2)$$

The same η is used for all the off-shell lines in all diagrams contributing to a given amplitude. In practice it will be convenient to choose $\eta^{\dot{a}}$ to be equal to $\tilde{\lambda}^{\dot{a}}$ of one of the external legs of negative helicity. External lines in a diagram remain on-shell, and for them λ is defined in the usual way.

Since in each MHV vertex (2.15) there are precisely two lines with negative helicities, and since a propagator always connects lines with opposite helicities, there is a simple relation between the number of negative helicity particles in a given amplitude and the number of MHV vertices needed to construct it,

$$q_{(-1)} + q_{(-\frac{1}{2})} = \sum v - 1 . \quad (3.3)$$

Here $q_{(-1)}$ is the number of negative helicity gluons, $q_{(-\frac{1}{2})}$ is the number of negative helicity fermions, and $\sum v$ is the total number of all MHV vertices (2.15) needed to construct this amplitude.

This formalism leads to explicit and relatively simple expressions for many amplitudes. n -point amplitudes with three particles of negative helicity is the next case beyond simple MHV amplitudes.

3.1 Calculating $- - - + + + \dots + +$ amplitudes with 2 fermions

To illustrate the power of the method in pure gauge theory, the authors of [2] have calculated n gluon amplitudes with three consecutive gluons of negative helicity $- - - + + + \dots + +$. In order to see precisely what is new when fermions are present, and to provide another useful application of the method, in this section we will calculate a similar amplitude with three negative helicities which are now carried by a fermion and two gluons.

We consider an n -point amplitude,

$$A_n(\Lambda_1^-, g_2^-, g_3^-, \Lambda_k^+) , \quad (3.4)$$

with one fermion and two gluons of negative helicities consecutive to each other, and a positive-helicity fermion in arbitrary position k , such that $3 < k \leq n$. As in the case considered in [2], this amplitude comes from scalar diagrams with two vertices and one propagator, but in our case there is more than one type of vertex in (2.15). There are three classes of scalar diagrams which contribute to $A_n(\Lambda_1^-, g_2^-, g_3^-, \Lambda_k^+)$, they are depicted in Figure 1. First two classes of diagrams involve the first and the second vertex in (2.15), and the third class involves two second vertices in (2.15).

First two diagrams in Figure 1 involve a gluon exchange. The third diagram involves a fermion exchange, and can be schematically represented as

$$A(\Lambda_1^-, g_2^-, \underline{\Lambda_I^+}) \frac{1}{q_I^2} A(g_3^-, \Lambda_k^+, \underline{\Lambda_{-I}^-}) . \quad (3.5)$$

Here $\underline{\Lambda_I^+}$ and $\underline{\Lambda_{-I}^-}$ denote internal off-shell fermions, which are Wick-contracted via the scalar propagator $1/q_I^2$. The order in which these internal fermion appear in (3.5) is according to the $\text{ket}^+ \text{ket}^-$ prescription discussed in the Appendix.

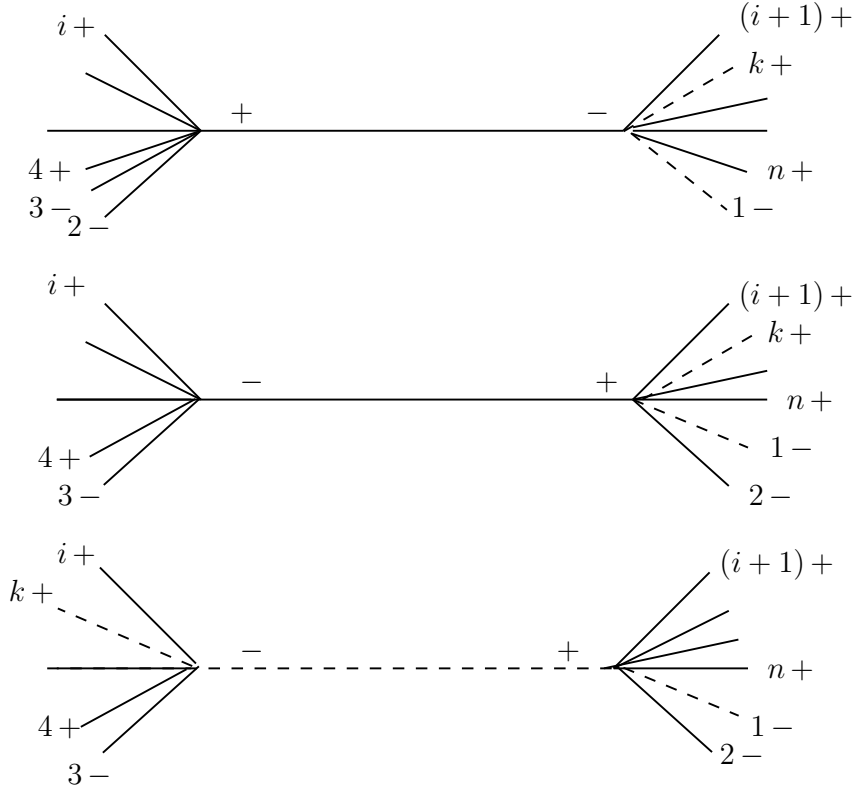


Figure 1: Tree diagrams with MHV vertices contributing to the $---++++\dots++$ amplitude with 2 fermions and $n-2$ gluons in Eq. (3.4). Fermions are represented by dashed lines and gluons – by solid lines.

The three diagrams in Figure 1 give

$$\begin{aligned}
A_n = & \sum_{i=3}^{k-1} \frac{\langle 1 (2, i) \rangle^2 \langle k (2, i) \rangle}{\langle (2, i) i+1 \rangle \langle i+1 i+2 \rangle \dots \langle n 1 \rangle} \frac{1}{q_{2i}^2} \frac{\langle 2 3 \rangle^3}{\langle (2, i) 2 \rangle \langle 3 4 \rangle \dots \langle i (2, i) \rangle} \\
& + \sum_{i=4}^{k-1} \frac{\langle 1 2 \rangle^2 \langle k 2 \rangle}{\langle 2 (3, i) \rangle \langle (3, i) i+1 \rangle \dots \langle n 1 \rangle} \frac{1}{q_{3i}^2} \frac{\langle (3, i) 3 \rangle^3}{\langle 3 4 \rangle \dots \langle i-1 i \rangle \langle i (3, i) \rangle} \\
& + \sum_{i=k}^n \frac{-\langle 1 2 \rangle^2}{\langle (3, i) i+1 \rangle \langle i+1 i+2 \rangle \dots \langle n 1 \rangle} \frac{1}{q_{3i}^2} \frac{\langle (3, i) 3 \rangle^2 \langle k 3 \rangle}{\langle 3 4 \rangle \dots \langle i-1 i \rangle \langle i (3, i) \rangle} .
\end{aligned} \tag{3.6}$$

Following notations of [2] we have introduced $q_{ij} = p_i + p_{i+1} + \dots + p_j$. The corresponding off-shell spinor λ_{ija} is defined as in (3.2), $\lambda_{ija} = q_{ija\dot{a}} \eta^{\dot{a}}$. All other spinors λ_i are on-shell and $\langle i (j, k) \rangle$ is an abbreviation for a spinor product $\langle \lambda_i, \lambda_{jk} \rangle$.

As in [2] we choose $\eta^{\dot{a}} = \tilde{\lambda}_2^{\dot{a}}$, and evaluate the amplitude (3.6) as a function of the on-shell kinematic variables, λ_i and $\tilde{\lambda}_1, \tilde{\lambda}_2, \tilde{\lambda}_3$. The final expression for the amplitude can

be written as the sum of three terms:

$$A_n = \frac{1}{\prod_{l=3}^n \langle l \ l+1 \rangle} [A_n^{(1)} + A_n^{(2)} + A_n^{(3)}] . \quad (3.7)$$

We have to treat the $i = 3$ term in the first sum in (3.6) and the $i = n$ term in the last sum in (3.6) separately, as individually they are singular for our choice of $\eta^{\dot{a}} = \tilde{\lambda}_2^{\dot{a}}$. These two terms are assembled into $A_n^{(3)}$.

For $i \neq 3$ the first and the second lines in (3.6) give

$$A_n^{(1)} = \sum_{i=4}^{k-1} \frac{\langle i \ i+1 \rangle}{\langle i^- | \not{q}_{2,i} | 2^- \rangle \langle (i+1)^- | \not{q}_{i+1,2} | 2^- \rangle \langle 2^- | \not{q}_{2,i} | 2^- \rangle} \cdot \left(\frac{\langle 3 \ 2 \rangle^3 \langle 1^- | \not{q}_{2,i} | 2^- \rangle^2 \langle k^- | \not{q}_{2,i} | 2^- \rangle}{q_{2,i}^2} + \frac{\langle 1 \ 2 \rangle^2 \langle k \ 2 \rangle \langle 3^- | \not{q}_{i+1,2} | 2^- \rangle^3}{q_{i+1,2}^2} \right) . \quad (3.8)$$

In evaluating (3.8) we used the Lorentz-invariant combination $\langle i^- | \not{p} | j^- \rangle = i^a p_{a\dot{a}} j^{\dot{a}}$, see Eq. (4.3) in the Appendix. We also used momentum conservation to set $q_{3,i} = -q_{i+1,2}$, and the anticommuting nature of spinor products to simplify the formula.

The second term in (3.7) is the contribution of the third line in (3.6) for $i \neq n$. We find

$$A_n^{(2)} = \sum_{i=k}^{n-1} \langle i \ i+1 \rangle \frac{1}{q_{i+1,2}^2} \frac{\langle 1 \ 2 \rangle^2 \langle k \ 3 \rangle \langle 3^- | \not{q}_{i+1,2} | 2^- \rangle^2}{\langle i^- | \not{q}_{i+1,2} | 2^- \rangle \langle (i+1)^- | \not{q}_{i+1,2} | 2^- \rangle} . \quad (3.9)$$

The remaining terms – the $i = 3$ term in the first sum in (3.6) and the $i = n$ term in the last sum in (3.6) – both contain a factor $[2 \ \eta]$ in the denominator and are singular for $|\eta^- \rangle = |2^- \rangle$. For the method to work, the singularity has to cancel between the two terms. This is indeed the case, and rather nontrivially the cancellation occurs between the diagrams of different types – the first and the last in Figure 1 – with different MHV vertices. After the singularity cancels, the remaining finite contribution from these two terms is derived by setting $|\eta^- \rangle = |2^- \rangle + |\epsilon^- \rangle$, bringing two terms to a common denominator and using Schouten's identity, $[\alpha \ \beta][\gamma \ \delta] + [\alpha \ \gamma][\delta \ \beta] + [\alpha \ \delta][\beta \ \gamma] = 0$. In the end $|\epsilon^- \rangle$ is set to zero. The result is

$$A_n^{(3)} = \langle 3 \ 1 \rangle \langle 3 \ k \rangle \left(\frac{s_{13} + 2(s_{12} + s_{23})}{[1 \ 2][2 \ 3]} + \frac{\langle 3 \ 1 \rangle \langle 2 \ n \rangle}{[1 \ 2] \langle 1 \ n \rangle} + \frac{\langle 3 \ 1 \rangle \langle 2 \ 4 \rangle}{[2 \ 3] \langle 3 \ 4 \rangle} - \frac{\langle 3 \ 1 \rangle \langle 2 \ k \rangle}{[2 \ 3] \langle 3 \ k \rangle} \right) \quad (3.10)$$

where $s_{km} = (p_k + p_m)^2 = \langle k \ m \rangle [k \ m]$.

3.2 Tests of the amplitude (3.7)–(3.10)

We will now test our result for an n -point $---+++\dots++$ amplitude with 2 fermions, against some known simple cases with $n = 4, 5$.

We first consider a 4-point amplitude with three negative helicities, $A_4(\Lambda_1^-, g_2^-, g_3^-, \Lambda_4^+)$ and check if this amplitude vanishes. Hence, we set $n = 4 = k$ and find that

$$A_n^{(1)} = 0, \quad A_n^{(2)} = 0, \quad (3.11)$$

since both expressions, (3.8) and (3.9), are proportional to $\sum_{i=4}^3 \equiv 0$. The remaining contribution $A_n^{(3)}$ in (3.10) gives

$$A_n^{(3)} = \langle 3\ 1 \rangle \langle 3\ k \rangle \left(-\frac{\langle 1\ 3 \rangle [1\ 3]}{[1\ 2][2\ 3]} + \frac{\langle 3\ 1 \rangle \langle 2\ 4 \rangle}{[1\ 2]\langle 1\ 4 \rangle} \right) = 0. \quad (3.12)$$

Here we first used that for $n = 4$ case $s_{12} + s_{23} + s_{13} = 0$, and a momentum conservation identity, $\langle 4\ 1 \rangle [1\ 3] + \langle 4\ 2 \rangle [2\ 3] = 0$.

The next test involves a 5-point amplitude with three negative helicities, $A_5(\Lambda_1^-, g_2^-, g_3^-, \Lambda_4^+, g_5^+)$. This is necessarily an $\overline{\text{MHV}}$ amplitude, or a mostly minus MHV amplitude which is (cf second equation in (2.18))

$$A_5(\Lambda_1^-, g_2^-, g_3^-, \Lambda_4^+, g_5^+) = -\frac{[5\ 4]^3 [5\ 1]}{\prod_{i=1}^5 [i\ i+1]} = \frac{[4\ 5]^2}{[1\ 2][2\ 3][3\ 4]}. \quad (3.13)$$

We set $n = 5, k = 4$ and evaluate expressions in (3.8)–(3.10). First, we notice again that

$$A_n^{(1)} = 0, \quad (3.14)$$

since $\sum_{i=4}^3 \equiv 0$. However, $A_n^{(2)}$ and $A_n^{(3)}$ are both non-zero,

$$\frac{A_n^{(2)}}{\prod_{l=3}^5 \langle l\ l+1 \rangle} = \frac{[4\ 2]^2 \langle 1\ 2 \rangle^2}{\langle 1\ 5 \rangle^2} \frac{1}{[1\ 2][2\ 3][3\ 4]}, \quad (3.15)$$

$$\frac{A_n^{(3)}}{\prod_{l=3}^5 \langle l\ l+1 \rangle} = \frac{\langle 3\ 1 \rangle}{\langle 4\ 5 \rangle \langle 5\ 1 \rangle} \left(2 \frac{\langle 4\ 5 \rangle [4\ 5]}{[1\ 2][2\ 3]} - \frac{\langle 1\ 3 \rangle [1\ 3]}{[1\ 2][2\ 3]} + \frac{\langle 3\ 1 \rangle \langle 2\ 5 \rangle}{[1\ 2]\langle 1\ 5 \rangle} \right) \quad (3.16)$$

We further use a momentum conservation identity to re-write the first factor in (3.15) as

$$\frac{[4\ 2]^2 \langle 1\ 2 \rangle^2}{\langle 1\ 5 \rangle^2} = \left([4\ 5] - \frac{\langle 1\ 3 \rangle [3\ 4]}{\langle 1\ 5 \rangle} \right)^2 = [4\ 5]^2 + \frac{\langle 1\ 3 \rangle^2 [3\ 4]^2}{\langle 1\ 5 \rangle^2} - 2 \frac{\langle 1\ 3 \rangle [3\ 4] [4\ 5]}{\langle 1\ 5 \rangle} \quad (3.17)$$

Now, the last term on the right hand side of (3.17) cancels the first term in brackets in (3.15) and the second term in (3.17) cancels the last two terms in (3.15) via an identity

$$[3\ 4]\langle 4\ 5\rangle + [3\ 1]\langle 1\ 5\rangle + [3\ 2]\langle 2\ 5\rangle = 0 . \quad (3.18)$$

The remaining $[4\ 5]^2$ term on the right hand side of (3.15) leads to the final answer for the amplitude,

$$\frac{[4\ 5]^2}{[1\ 2][2\ 3][3\ 4]} . \quad (3.19)$$

We expect that other, more involved tests of the amplitude at the 6-point level and beyond will also be successful.

3.3 Calculating $---++++\dots++++$ amplitudes with 4 fermions

Since the scalar graph method gives correct results for non-MHV amplitudes with 2 external fermions, the next step is to apply this method to 4-fermion amplitudes. In this section we will calculate an n -point amplitude with 4 fermions for three negative helicities consecutive to each other,

$$A_n(g_1^-, \Lambda_2^-, \Lambda_3^-, \Lambda_p^+, \Lambda_q^+) , \quad (3.20)$$

where $3 < p < q \leq n$. As always, positive-helicity gluons in amplitudes will not be indicated explicitly, unless they appear in internal lines.

There are four scalar diagrams which contribute to this process. They are drawn in Figure 2. The first diagram in Figure 2 is a gluon exchange between two 2-fermion MHV-vertices. This diagram has a schematic form,

$$A(g_1^-, \Lambda_2^-, \underline{g_I^+}, \Lambda_q^+) \frac{1}{q_I^2} A(\Lambda_3^-, \Lambda_p^+, \underline{g_{-I}^-}) . \quad (3.21)$$

Here $\underline{g_I^+}$ and $\underline{g_{-I}^-}$ are off-shell (internal) gluons which are Wick-contracted via a scalar propagator, and $I = (3, i)$.

The second diagram involves a gluon exchange between a 0-fermion and a 4-fermion MHV vertex,

$$A(g_1^-, \underline{g_I^-}) \frac{1}{q_I^2} A(\Lambda_2^-, \Lambda_3^-, \Lambda_p^+, \Lambda_q^+, \underline{g_{-I}^+}) , \quad (3.22)$$

with external index $I = (2, i)$. Note that this diagram exists only for $n > 5$, i.e. there must be at least one g^+ in the first vertex, otherwise it is a 2-point vertex which does not exist.

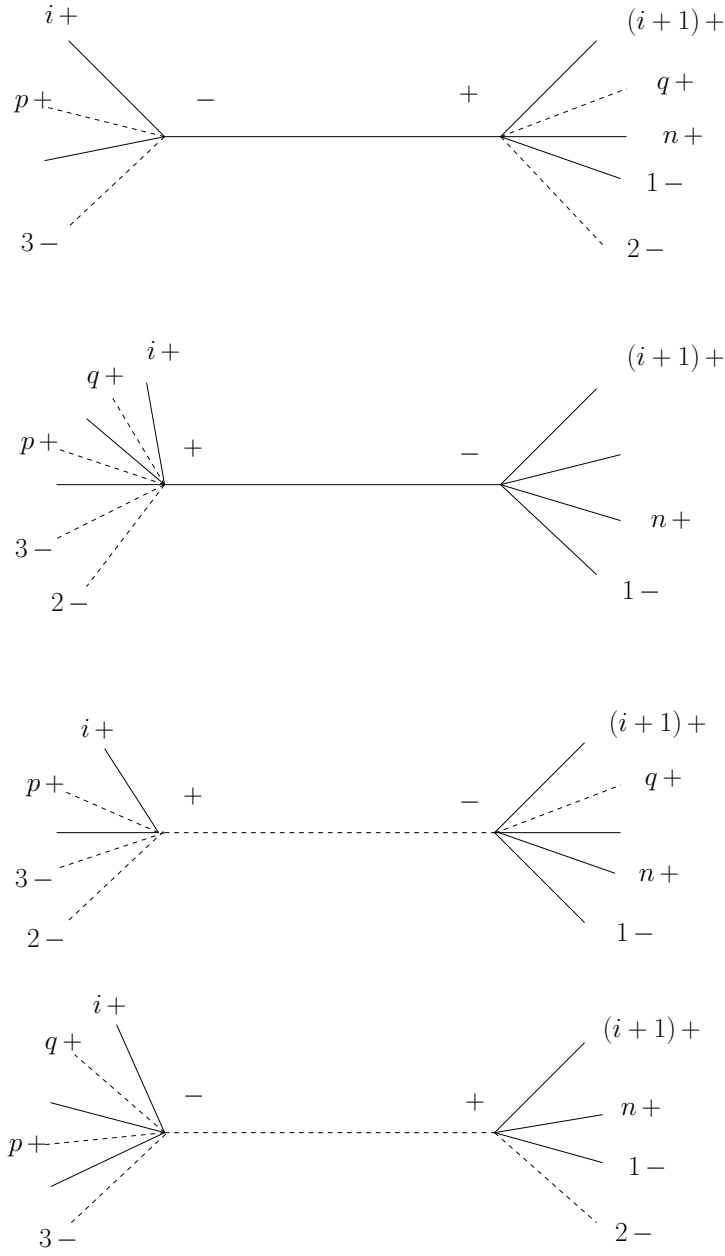


Figure 2: *Diagrams contributing to the 4-fermion n -point amplitude (3.20)*

The third and the fourth diagrams in Figure 2 involve a fermion exchange between a 2-fermion and a 4-fermion MHV vertices. They are given, respectively by

$$A(\Lambda_2^-, \Lambda_3^-, \Lambda_p^+, \underline{\Lambda_{-I}^+}) \frac{1}{q_I^2} A(\Lambda_q^+, g_1^-, \underline{\Lambda_I^-}) , \quad (3.23)$$

with $I = (2, i)$, and

$$A(g_1^-, \Lambda_2^-, \underline{\Lambda_I^+}) \frac{1}{q_I^2} A(\Lambda_3^-, \Lambda_p^+, \Lambda_q^+, \underline{\Lambda_{-I}^-}) , \quad (3.24)$$

with $I = (3, i)$. Both expressions, (3.23) and (3.24), are written in the form which is in agreement with our ordering prescription for internal fermions, $\text{ket}^+ \text{ket}^-$.

We will continue using the same off-shell prescription $\eta^{\dot{a}} = \tilde{\lambda}_2^{\dot{a}}$ as in the section **3.1**. But there is an important simplification in the present case compared to **3.1** – there will be no singular terms appearing in individual diagrams. This is because the reference spinor $\eta^{\dot{a}} = \tilde{\lambda}_2^{\dot{a}}$ now corresponds to a gluino, rather than a gluon g^- . The reason for singularities encountered in section **3.1** and in Ref. [2] was simply the singular collinear limit of the 3-gluon vertex where all gluons went on-shell. We will see that these singularities would not occur in the present case, and not having to cancel them will save us some work.⁵

For extra clarity we will first present a simpler version of the evaluation of (3.20) for the case $n = 5$. This result will then be generalized to all values of n . For $n = 5$, we set $p = 4$ and $q = 5$ in (3.20), and the calculation is straightforward.

1. The first diagram in Figure 2, Eq. (3.21), is

$$\begin{aligned} & \frac{-\langle 1\ 2 \rangle^2}{(\langle 2\ 3 \rangle [2\ 3] + \langle 2\ 4 \rangle [2\ 4]) \langle 5\ 1 \rangle [2\ 1]} \cdot \frac{1}{\langle 3\ 4 \rangle [3\ 4]} \cdot \langle 4\ 3 \rangle [2\ 4]^2 \\ &= \frac{[2\ 4]^2 \langle 1\ 2 \rangle^2}{[3\ 4] (\langle 2\ 3 \rangle [2\ 3] + \langle 2\ 4 \rangle [2\ 4]) \langle 5\ 1 \rangle [2\ 1]} . \end{aligned} \quad (3.25)$$

2. The second diagram is zero.

3. The third diagram, Eq. (3.23), is

$$\begin{aligned} & \frac{-\langle 2\ 3 \rangle^2}{(\langle 2\ 3 \rangle [2\ 3] + \langle 2\ 4 \rangle [2\ 4]) \langle 3\ 4 \rangle} \cdot \frac{1}{\langle 5\ 1 \rangle [5\ 1]} \cdot \frac{\langle 5\ 1 \rangle [2\ 5]^2}{[2\ 1]} \\ &= \frac{-[2\ 5]^2 \langle 2\ 3 \rangle^2}{[2\ 1] [5\ 1] (\langle 2\ 3 \rangle [2\ 3] + \langle 2\ 4 \rangle [2\ 4]) \langle 3\ 4 \rangle} . \end{aligned} \quad (3.26)$$

⁵In view of this, the calculation in section **3.1** could have been made simpler, if we had chosen the reference spinor to be the spinor of the negative-helicity gluino Λ_1^- .

4. The fourth diagram, Eq. (3.24):

$$\frac{\langle 2\ 1 \rangle}{[2\ 1]} \cdot \frac{1}{\langle 1\ 2 \rangle [1\ 2]} \cdot \frac{\langle 3\ 1 \rangle^2 [2\ 1]}{\langle 3\ 4 \rangle \langle 5\ 1 \rangle} = \frac{\langle 3\ 1 \rangle^2}{[2\ 1] \langle 3\ 4 \rangle \langle 5\ 1 \rangle} . \quad (3.27)$$

Now, we need to add up the three contributions. We first combine the expressions in (3.25) and (3.26) into

$$\frac{[4\ 5]^2}{[2\ 1][3\ 4][5\ 1]} - \frac{\langle 3\ 1 \rangle^2}{[2\ 1]\langle 3\ 4 \rangle \langle 5\ 1 \rangle} \quad (3.28)$$

using momentum conservation identities, and the fact that $\langle 2\ 3 \rangle [2\ 3] + \langle 2\ 4 \rangle [2\ 4] = -\langle 3\ 4 \rangle [3\ 4] + \langle 5\ 1 \rangle [5\ 1]$. Then, adding the remaining contribution (3.27) we obtain the final result for the amplitude,

$$A_5(g_1^-, \Lambda_2^-, \Lambda_3^-, \Lambda_4^+, \Lambda_5^+) = \frac{-[4\ 5]^3 [2\ 3]}{[1\ 2][2\ 3][3\ 4][4\ 5][5\ 1]} . \quad (3.29)$$

which is the precisely right answer for the MHV-bar 5-point ‘mostly minus’ diagram!

We now present the general expression for the amplitude with n external legs. Using the same prescription for the vertices as above the first diagram of Figure 2 gives

$$\begin{aligned} A_n^{(1)} &= \sum_{i=p}^{q-1} \frac{\langle 1\ 2 \rangle^2 \langle 1\ q \rangle}{\langle 2\ (3, i) \rangle \langle (3, i)\ i+1 \rangle \langle i+1\ i+2 \rangle \dots \langle n\ 1 \rangle} \frac{1}{q_{3i}^2} \frac{\langle 3\ -(3, i) \rangle^3 \langle p\ -(3, i) \rangle}{\langle 3\ 4 \rangle \dots \langle i\ -(3, i) \rangle \langle -(3, i)\ 3 \rangle} \\ &= -\frac{1}{\prod_{l=3}^n \langle l\ l+1 \rangle} \sum_{i=p}^{q-1} \frac{\langle 1\ 2 \rangle^2 \langle 1\ q \rangle \langle i\ i+1 \rangle \langle 3^- | \not{\epsilon}_{i+1,2} | 2^- \rangle^2 \langle p^- | \not{\epsilon}_{2,i} | 2^- \rangle}{q_{i+1,2}^2 \langle i^- | \not{\epsilon}_{2,i} | 2^- \rangle \langle (i+1)^- | \not{\epsilon}_{i+1,2} | 2^- \rangle \langle 2^- | \not{\epsilon}_{2,i} | 2^- \rangle} . \end{aligned} \quad (3.30)$$

For the second diagram of Figure 2 one obtains

$$\begin{aligned} A_n^{(2)} &= \sum_{i=q}^{n-1} \frac{\langle 1\ (2, i) \rangle^3}{\langle (2, i)\ i+1 \rangle \langle i+1\ i+2 \rangle \dots \langle n\ 1 \rangle} \frac{1}{q_{2,i}^2} \frac{-\langle 2\ 3 \rangle^2 \langle p\ q \rangle}{\langle 3\ 4 \rangle \dots \langle i\ -(2, i) \rangle \langle -(2, i)\ 2 \rangle} \\ &= \frac{1}{\prod_{l=3}^n \langle l\ l+1 \rangle} \sum_{i=q}^{n-1} \frac{\langle 2\ 3 \rangle^2 \langle p\ q \rangle \langle i\ i+1 \rangle \langle 1^- | \not{\epsilon}_{2,i} | 2^- \rangle^3}{q_{2,i}^2 \langle i^- | \not{\epsilon}_{2,i} | 2^- \rangle \langle (i+1)^- | \not{\epsilon}_{i+1,2} | 2^- \rangle \langle 2^- | \not{\epsilon}_{2,i} | 2^- \rangle} . \end{aligned} \quad (3.31)$$

The contribution of the third diagram of Figure 2 is

$$\begin{aligned} A_n^{(3)} &= \sum_{i=p}^{q-1} -\frac{\langle 1\ (2, i) \rangle^2 \langle 1\ q \rangle}{\langle (2, i)\ i+1 \rangle \langle i+1\ i+2 \rangle \dots \langle n\ 1 \rangle} \frac{1}{q_{2,i}^2} \frac{-\langle 2\ 3 \rangle^2 \langle p\ -(2, i) \rangle}{\langle 3\ 4 \rangle \dots \langle i\ -(2, i) \rangle \langle -(2, i)\ 2 \rangle} \\ &= \frac{1}{\prod_{l=3}^n \langle l\ l+1 \rangle} \sum_{i=p}^{q-1} \frac{\langle 2\ 3 \rangle^2 \langle 1\ q \rangle \langle i\ i+1 \rangle \langle p^- | \not{\epsilon}_{2,i} | 2^- \rangle \langle 1^- | \not{\epsilon}_{2,i} | 2^- \rangle^2}{q_{2,i}^2 \langle i^- | \not{\epsilon}_{2,i} | 2^- \rangle \langle (i+1)^- | \not{\epsilon}_{i+1,2} | 2^- \rangle \langle 2^- | \not{\epsilon}_{2,i} | 2^- \rangle} . \end{aligned} \quad (3.32)$$

Finally, from the fourth diagram of Figure 2 we get

$$\begin{aligned}
A_n^{(4)} &= \sum_{i=q}^n \frac{\langle 1 \ 2 \rangle^2 \langle 1 \ (3, i) \rangle}{\langle 2 \ (3, i) \rangle \langle (3, i) \ i+1 \rangle \langle i+1 \ i+2 \rangle \dots \langle n \ 1 \rangle} \frac{1}{q_{3,i}^2} \frac{-\langle 3 \ - (3, i) \rangle^3 \langle p \ q \rangle}{\langle 3 \ 4 \rangle \dots \langle i \ - (3, i) \rangle \langle -(3, i) \ 3 \rangle} \\
&= -\frac{1}{\prod_{l=3}^n \langle l \ l+1 \rangle} \sum_{i=q}^n \frac{\langle 1 \ 2 \rangle^2 \langle p \ q \rangle \langle i \ i+1 \rangle \langle 3^- | \not{q}_{i+1,2} | 2^- \rangle^2 \langle 1^- | \not{q}_{2,i} | 2^- \rangle}{q_{i+1,2}^2 \langle i^- | \not{q}_{2,i} | 2^- \rangle \langle (i+1)^- | \not{q}_{i+1,2} | 2^- \rangle \langle 2^- | \not{q}_{2,i} | 2^- \rangle} .
\end{aligned} \tag{3.33}$$

One can combine the result for the first and the third diagram to get:

$$A_n^{(1,3)} = \frac{1}{\prod_{l=3}^n \langle l \ l+1 \rangle} \sum_{i=p}^{q-1} \frac{\langle 1 \ q \rangle \langle i \ i+1 \rangle \langle p^- | \not{q}_{2,i} | 2^- \rangle}{\langle i^- | \not{q}_{2,i} | 2^- \rangle \langle (i+1)^- | \not{q}_{i+1,2} | 2^- \rangle \langle 2^- | \not{q}_{2,i} | 2^- \rangle} \tag{3.34}$$

$$\cdot \left(-\frac{\langle 1 \ 2 \rangle^2 \langle 3^- | \not{q}_{i+1,2} | 2^- \rangle^2}{q_{i+1,2}^2} + \frac{\langle 2 \ 3 \rangle^2 \langle 1^- | \not{q}_{2,i} | 2^- \rangle^2}{q_{2,i}^2} \right) . \tag{3.35}$$

The final result for the n -point amplitude is with 4 fermions

$$A_n(g_1^-, \Lambda_2^-, \Lambda_3^-, \Lambda_p^+, \Lambda_q^+) = A_n^{(1,3)} + A_n^{(2)} + A_n^{(4)} . \tag{3.36}$$

All the individual terms are regular, and the equation above is the final result of this section.

4 Loop Amplitudes and IR Divergencies

An intriguing question is how to go beyond the tree level. There are some obvious conceptual problems in trying to work with loop amplitudes, directly in 4 dimensions and without an infrared cutoff (e.g. in the superconformal $\mathcal{N} = 4$ SYM). Loop amplitudes in massless gauge theories suffer from severe infrared (IR) – soft and collinear – divergencies. At tree-level there are no integrations over loop momenta and IR divergencies in the amplitudes can be avoided by selecting a non-exceptional set of external momenta (i.e the set with none of the external momenta being collinear or soft). Hence tree amplitudes can be made IR finite and it is meaningful to be calculating them directly in 4D without an explicit IR cutoff.

Loop amplitudes, however, are always IR divergent, in other words, one cannot choose a set of external momenta which would make an on-shell loop amplitude finite in 4D. These IR divergencies simply reflect the fact that the naive S-matrix and scattering amplitudes simply do not exist in a gauge theory with massless particles. In QCD (and QED)

this problem is avoided either by calculating cross-sections directly or by defining new asymptotic initial and final states with indefinite numbers of massless quarks and gluons. The Kinoshita-Lee-Nauenberg theorem states that all the IR divergencies cancel (collinear with collinear, soft with soft) in properly defined physical observables, when one sums over degenerate initial as well as final states.

In the superconformal $\mathcal{N} = 4$ theory the situation is less clear. Well-defined observables of this theory are not the amplitudes, but Green functions of gauge-invariant composite operators, and the latter were used successfully in the context of the AdS/CFT correspondence.

It would be very interesting to understand better what are the relevant infrared-safe quantities in a 4-dimensional gauge theory which can be deduced from a dual string theory in twistor space.

Acknowledgements

VVK would like to thank participants of ‘Strings, Gauge Fields and Duality’ conference in Swansea, where this work was started, for useful conversations. He is also grateful to Adrian Signer for comments. VVK is supported in part by a PPARC Senior Research Fellowship. GG acknowledges a grant from the State Scholarship Foundation of Greece (I.K.Y.)

Appendix: Note on Spinor Conventions

Spinor products are defined as

$$\langle i \ j \rangle \equiv \langle i^- | j^+ \rangle = \lambda_i^a \lambda_{j\ a} , \quad [i \ j] \equiv \langle i^+ | j^- \rangle = \tilde{\lambda}_i^{\dot{a}} \tilde{\lambda}_{j\ \dot{a}} . \quad (4.1)$$

Here spinor indices are raised and lowered with ϵ -symbols, and we follow the sign conventions of [1, 2]. It should be noted, that slightly different sign conventions from (4.1) have been used in earlier literature for $[i \ j]$. For example, in [12] the dotted spinor product, $[i \ j]$, is defined as $\tilde{\lambda}_i^{\dot{a}} \tilde{\lambda}_{j\ \dot{a}} = -\tilde{\lambda}_i^{\dot{a}} \tilde{\lambda}_{j\ \dot{a}}$. In conventions of [12], equation (2.9) would have a minus sign on the right hand side.

An on-shell momentum of a massless particle, p_k^μ can be written as

$$p_{k\ a\dot{a}} = p_{k\mu} \sigma^\mu = \lambda_{k\ a} \tilde{\lambda}_{k\ \dot{a}} . \quad (4.2)$$

In section 3 we use a Lorentz-invariant combination $\langle i^- | \not{p}_k | j^- \rangle = i^a p_{k\ a\dot{a}} j^{\dot{a}}$, which in terms of the spinor products (4.1) is

$$\langle i^- | \not{p}_k | j^- \rangle = \langle i^- |^a | k^+ \rangle_a \langle k^+ |_{\dot{a}} | j^- \rangle^{\dot{a}} = -\langle i \ k \rangle [k \ j] = \langle i \ k \rangle [j \ k] . \quad (4.3)$$

The spinors λ and $\tilde{\lambda}$ appearing in the helicity formalism are precisely the wave-functions of fermions of positive and negative helicities,

$$\begin{aligned} \langle i^- |^a &= \lambda_i^a = \overline{u}_-(k_i)^a , & |i^+ \rangle_a &= \lambda_{i\ a} = u_+(k_i)_a , \\ \langle i^+ |^{\dot{a}} &= \tilde{\lambda}_i^{\dot{a}} = \overline{u}_+(k_i)^{\dot{a}} , & |i^- \rangle_{\dot{a}} &= \tilde{\lambda}_{i\ \dot{a}} = u_-(k_i)_{\dot{a}} . \end{aligned} \quad (4.4)$$

In our conventions for MHV vertices we treat all fermions and antifermions as incoming and the fermion propagator connects two incoming fermions with opposite helicities. Thus, the completeness relation relevant for us and with a correct index structure gives

$$\frac{|i^+ \rangle_a |i^- \rangle_{\dot{a}}}{k_i^2} = \frac{\lambda_{i\ a} \tilde{\lambda}_{i\ \dot{a}}}{k_i^2} = \frac{k_{i\ a\dot{a}}}{k_i^2} , \quad (4.5)$$

which is, of course, the correct fermion propagator in usual Feynman perturbation theory.

Scalars have no wave-functions, and their propagator remains $1/k^2$, and vectors give (in Feynman gauge)

$$\frac{\varepsilon_+^\mu \varepsilon_-^\nu}{k^2} = \frac{-g^{\mu\nu}}{k^2} , \quad (4.6)$$

which is the correct form of the massless vector boson propagator.

An important consequence of (4.5) is the ordering prescription of fermions in MHV vertices. This concerns only the case of scalar diagrams with internal fermion lines, such as the third diagram in Figure 1. In this case, in order to get the $\text{ket}^+ \text{ket}^-$ structure $|i^+\rangle_a | - i^-\rangle_{\dot{a}}$ the two fermions which are to be connected by a propagator should be both on the right of each vertex (rather than adjacent to each other). This means that, for example, the third diagram in Figure 1 comes from

$$A(\Lambda_1^-, g_2^-, \underline{\Lambda_{(3i)}^+}) A(g_3^-, \Lambda_k^+, \underline{\Lambda_{-(3i)}^-}) . \quad (4.7)$$

If the contracted fermion factors, $\underline{\Lambda_{(3i)}^+}$ and $\underline{\Lambda_{-(3i)}^-}$ were, instead, chosen to be next to each other, the overall contribution would change sign, since fermions anticommute with each other.

References

- [1] E. Witten, “Perturbative gauge theory as a string theory in twistor space,” hep-th/0312171.
- [2] F. Cachazo, P. Svrcek and E. Witten, “MHV vertices and tree amplitudes in gauge theory,” hep-th/0403047.
- [3] C. J. Zhu, “The googly amplitudes in gauge theory,” hep-th/0403115.
- [4] F. A. Berends and W. T. Giele, “Recursive Calculations For Processes With N Gluons,” Nucl. Phys. B **306** (1988) 759.
- [5] D. A. Kosower, “Light Cone Recurrence Relations For QCD Amplitudes,” Nucl. Phys. B **335** (1990) 23.
- [6] G. Chalmers and W. Siegel, “Simplifying algebra in Feynman graphs. II: Spinor helicity from the spacecone,” Phys. Rev. D **59** (1999) 045013, hep-ph/9801220; W. Siegel, “Fields,” hep-th/9912205.
- [7] R. Roiban, M. Spradlin and A. Volovich, “A googly amplitude from the B-model in twistor space,” hep-th/0402016;
R. Roiban and A. Volovich, “All googly amplitudes from the B-model in twistor space,” hep-th/0402121;
R. Roiban, M. Spradlin and A. Volovich, “On the tree-level S-matrix of Yang-Mills theory,” hep-th/0403190.

- [8] Work in progress.
- [9] M. L. Mangano and S. J. Parke, “Multiparton Amplitudes In Gauge Theories,” Phys. Rept. **200** (1991) 301.
- [10] F. A. Berends, R. Kleiss, P. De Causmaecker, R. Gastmans and T. T. Wu, Phys. Lett. B **103** (1981) 124;
P. De Causmaecker, R. Gastmans, W. Troost and T. T. Wu, Nucl. Phys. B **206** (1982) 53;
R. Kleiss and W. J. Stirling, Nucl. Phys. B **262** (1985) 235;
J. F. Gunion and Z. Kunszt, Phys. Lett. B **161** (1985) 333.
- [11] S. J. Parke and T. R. Taylor, “An Amplitude For N Gluon Scattering,” Phys. Rev. Lett. **56** (1986) 2459.
- [12] L. J. Dixon, “Calculating scattering amplitudes efficiently,” hep-ph/9601359.
- [13] V. P. Nair, “A Current Algebra For Some Gauge Theory Amplitudes,” Phys. Lett. B **214** (1988) 215.